Oscillator strengths and line widths of dipole-allowed transitions in $^{14}N_2$ between 86.0 and 89.7 nm

A. N. Heays,[1,a)] B. R. Lewis,[1] G. Stark,[2] K. Yoshino,[3] Peter L. Smith,[3] K. P. Huber,[4] and K. Ito[5]

[1]*Research School of Physical Sciences and Engineering, The Australian National University, Canberra, Australian Capital Territory 0200, Australia*
[2]*Department of Physics, Wellesley College, Wellesley, Massachusetts 02481, USA*
[3]*Harvard-Smithsonian Center for Astrophysics, Cambridge, Massachusetts 02138, USA*
[4]*Steacie Institute for Molecular Sciences, National Research Council of Canada, Ottawa, Ontario K1A 0R6, Canada*
[5]*Photon Factory, Institute for Materials Structure Science, High Energy Accelerator Research Organization, 1-1 Oho, Tsukuba, Ibaraki 305-0801, Japan*

(Received 18 August 2009; accepted 10 October 2009; published online 20 November 2009)

Oscillator strengths of 23 electric-dipole-allowed bands of $^{14}N_2$ in the 86.0–89.7 nm (111 480–116 280 cm^{-1}) region are reported from synchrotron-based photoabsorption measurements at an instrumental resolution of 6.5×10^{-4} nm (0.7 cm^{-1}) full width at half maximum. The absorption spectrum comprises transitions to vibrational levels of the $c_n\ ^1\Pi_u$ $(n=3,4)$, $o_3\ ^1\Pi_u$, and $c'_{n+1}\ ^1\Sigma_u^+(n=3,4)$ Rydberg states as well as the $b\ ^1\Pi_u$ and $b'\ ^1\Sigma_u^+$ valence states. The J dependences of band f-values derived from the experimental line f-values are reported as polynomials in $J(J+1)$ and are extrapolated to zero nuclear rotation in order to facilitate comparisons with the results of coupled Schrödinger equation calculations. Many bands in this study are characterized by a strong J dependence of the band f-values and display anomalous P-, Q-, and R-branch intensity patterns. Predissociation line widths are reported for six bands. The experimental f-value and line-width patterns inform current efforts to develop comprehensive spectroscopic models for N_2 that incorporate rotational effects and predissociation mechanisms, and are critical for the construction of realistic atmospheric radiative-transfer models. © *2009 American Institute of Physics*. [doi:10.1063/1.3257690]

I. INTRODUCTION

The excitation of molecular nitrogen and its subsequent dissociation are important drivers of the chemical dynamics in the upper atmosphere of the Earth and in other nitrogen-rich planetary atmospheres. For example, airglow emission in the extreme-ultraviolet and vacuum-ultraviolet spectral regions, attributable to N_2 following photoexcitation or electron-impact excitation, has been observed terrestrially[1,2] and in the atmospheres of Titan[3–5] and Triton.[6] In all cases, difficulties remain in the interpretation of the observations and in the understanding of the resulting chemical and radiative dynamics. More generally, the modeling of many upper-atmospheric photochemical processes[7–11] requires a detailed understanding of the photoabsorption spectrum of $^{14}N_2$ and its isotopic variants.

The onset of the electric-dipole-allowed absorption spectrum from the $X\ ^1\Sigma_g^+$ ground state of N_2 occurs near 100 nm, with all dipole-accessible excited levels lying above the first dissociation limit and subject to predissociation. The patterns of vibronic spacings, line widths and absorption oscillator strengths for the excited levels of N_2 are highly erratic. The main irregularities of the spectrum were first explained successfully[12–14] by invoking strong interactions between two valence states, $b\ ^1\Pi_u$ and $b'\ ^1\Sigma_u^+$, and three Rydberg series: the $np\sigma$ and $np\pi$ series converging to the $X\ ^2\Sigma_g^+$ ground state of the ion, and the $ns\sigma$ series converging to the first excited state $A\ ^2\Pi_u$. In the following, we refer to the Rydberg states using the traditional labels c'_{n+1} and c_n for, respectively, the Σ and Π components of a p-complex, and o_n for a core-excited Π state.

The homogeneous interactions between these states, $^1\Pi_u\sim{}^1\Pi_u$ and $^1\Sigma_u^+\sim{}^1\Sigma_u^+$, were studied in detail by Stahel *et al.*,[15] who employed a coupled-channels model constrained by an experimental database of vibronic term values, rotational constants, and relative dipole strengths determined from electron energy-loss spectra.[16] Rotational interactions between $^1\Pi_u$ and $^1\Sigma_u^+$ states were not incorporated in this model. Spelsberg and Meyer[17] refined the analysis of Stahel *et al.*[15] by employing *ab initio* potential energy curves and internuclear distance-dependent electronic-coupling parameters and transition moments, optimized to reproduce laboratory measurements.

A coupled-channels Schrödinger equation (CSE) model taking into account the interactions between $b\ ^1\Pi_u$, $c_3\ ^1\Pi_u$, and $o_3\ ^1\Pi_u$, and the $^3\Pi_u$ valence states C and C', was developed by Lewis *et al.*,[18] clarifying the predominant indirect predissociation mechanism affecting the photoabsorption spectrum. Their model demonstrated that the spin-orbit interaction between the $b\ ^1\Pi_u$ and $C\ ^3\Pi_u$ states, along with an electrostatic interaction between $C\ ^3\Pi_u$ and the continuum of

a)Electronic mail: alan.heays@anu.edu.au.

$C'\ ^3\Pi_u$, accounts for the line-broadening patterns observed shortward of 95 nm.[19–21] Haverd *et al.*[22] extended the CSE model of Lewis *et al.*[18] to reproduce the measured rotational effects[20] on line strengths and predissociation line widths for the lowest-energy $^1\Pi_u - X\ ^1\Sigma_g^+$ vibrational bands. The recent inclusion of the F and $G\ ^3\Pi_u$ Rydberg states[23–25] has enabled an extension of the CSE model to higher transition energies.[26] The incorporation into the model of heterogeneous interactions with the $c_n'\ ^1\Sigma_u^+$ and $b'\ ^1\Sigma_u^+$ states, informed by the laboratory measurements reported herein, is currently underway. Liu *et al.*[27] and Khakoo *et al.*[28] have reported applications of the CSE model to the interpretation of electron-impact excitation spectra.

Early optical measurements[29,30] of N_2 band oscillator strengths suffered from saturation effects associated with insufficient spectral resolution.[31] Electron-scattering measurements are not subject to saturation effects but, due to their inferior spectral resolution, require the deconvolution of highly blended features in the extraction of band f-values. Geiger and Schröder[16] reported relative intensities in the N_2 energy-loss spectrum of 25 keV electrons at a resolution of 10 meV full width at half maximum (FWHM) and Chan *et al.*[32] determined N_2 band f-values from energy-loss spectra of 8 keV electrons at a resolution of 48 meV FWHM.

Predissociation line broadening is generally less pronounced in the absorption bands shortward of 90 nm than in those reported previously at longer wavelengths.[20,21,33–35] While there is no comprehensive line-width database, there have been laser-based measurements of a few selected bands in this region[36–38] as well as photofragment studies[39–42] that reveal predissociation yields and dissociation product branching ratios.

The strong homogeneous and rotational interactions among the singlet and triplet states of N_2 can produce striking rotation-dependent effects on line strengths and widths. Within the spectral region studied in this report, Helm *et al.*[36] reported the rotational dependence of line widths in the $c_4'(4)$ and $c_3(4)-X(0)$ bands, and Helm and Cosby[39] and Walter *et al.*[40–42] reported departures from normal rovibrational intensity patterns in photofragment signals following laser excitation of the $c_4'(4)$, $c_3(4)$, $c_5'(0)$, and $c_4(0)$ levels, as well as a number of $b'(v)$ levels. Heterogeneous interactions are responsible for many of the rotation-dependent effects. In their interpretation of the photofragment signals, Helm and Cosby[39] applied a local deperturbation analysis to six coupled vibronic levels, while Helm *et al.*[36] and Walter *et al.*[42] extended the coupled-channels treatment of Stahel *et al.*[15] by including the effects of rotation to interpret the observed J-dependences of photofragment intensities and predissociation yields.

The present work is a continuation of our measurement program[20,21] to survey at high resolution the dipole-allowed photoabsorption spectrum of $^{14}N_2$ from its onset to the first ionization limit at 79.6 nm. We report line oscillator strength and predissociation line-width measurements for 23 vibronic bands of N_2 in the 86.0–89.7 nm (111 480–116 280 cm^{-1}) region. The bands studied include transitions between the ground state $X(0)$ and the vibronic upper states $b(15-20,22-23)$, $b'(12-18)$, $c_3(4-5)$, $o_3(4-5)$, $c_4(0)$, $c_4'(4-5)$, and $c_5'(0)$.

II. EXPERIMENTAL PROCEDURE AND ANALYSIS

Detailed descriptions of the experiment, analysis procedure, and sources of uncertainty have been given previously,[20,21] and are summarized here. Measurements were undertaken at the Photon Factory synchrotron radiation facility in Tsukuba, Japan. A 6.65 m grating spectrometer provided an instrumental resolution of $\sim 6\times 10^{-4}$ nm (~ 0.7 cm^{-1}) FWHM and served as an absorption cell with a path length of 12.5 m. Room temperature photoabsorption spectra were recorded at N_2 column densities ranging from 4.1×10^{13} to 4.9×10^{15} cm^{-2} with a signal-to-noise ratio of ~ 250.

Absorption features were fitted numerically using a least-squares program. Each line was represented by a Voigt profile, with a fixed Doppler component and free parameters representing transition energy, strength, and natural line width. The instrument function was represented by a Gaussian of width 0.65 cm^{-1} FWHM, determined by fitting the narrowest measured lines assuming negligible natural line width.

A database of N_2 transition energies,[43] compiled from photographic absorption experiments, provides a basis for wavelength calibration. The present work has enabled, in some cases, an improved energy assignment of blended or perturbed lines. Wholly new rotational assignments have been made for the bands $b(20)-$, $c_3(5)-$, $c_4'(5)-$, and $o_3(5)-X(0)$.

Line f-values, determined from the fitting procedure, were converted into band f-values using standard Hönl–London factors for $^1\Sigma-{}^1\Sigma$ and $^1\Pi-{}^1\Sigma$ transitions.[44] Most bands in this study display anomalous P-, Q-, and R-branch intensity patterns and are characterized by a marked rotational dependence of band f-values. It is the upper-state wave function that is primarily responsible for these variations and, accordingly, the band f-values measured here are indexed by J', the upper-state angular-momentum quantum number.

The J'-dependences of the measured band f-values and predissociation line widths are modeled as simple polynomials and extrapolated to zero nuclear rotation, allowing direct comparison with CSE molecular models[15,17,18] that do not account for rotational effects.

The uncertainties in individual line f-values from all sources, including statistical uncertainties of the fitted parameters (typically 10%) and systematic uncertainty in the spectrometer column density ($\sim 10\%$), are estimated to range from 10% to 30% (1 standard error). Line width uncertainties are $\gtrsim 15\%$ and vary widely.

III. RESULTS AND DISCUSSION

Summaries of our f-value and line-width measurements are presented in Tables I and II, respectively. A detailed listing of experimental f-values and widths for individual rotational lines can be accessed through the EPAPS data deposi-

TABLE I. Summary of band f-values (in units of 10^{-3}). Uncertainties in units of the last significant digit are given in parentheses.

Band	T_0 [a] (cm^{-1})	f_0 [b]	$f(J')$ [c] $0 \le J' \le J'_{max}$	No. lines[d]	Obs. J' [e]	J'_{max} [f]
$b(15)-X(0)$	111 872	<1	1.9	4	15–20	
$b'(12)$	112 238	16(2)	$16-4.6\times10^{-3}x$	38	0–21	
$b(16)$	112 509	1.1(2)	1.1	6	2–9	
$c'_4(4)$	112 768	18(2)	$18+6.0\times10^{-2}x-1.1\times10^{-4}x^2$	35	1–23	
$c_3(4)$	112 851	<0.3	$P,R: 0+4.1\times10^{-3}x+2.2\times10^{-3}x^2$	15	3–15	8
$b'(13)$	112 908	10(1)	$10.0-1.3\times10^{-1}x+4.2\times10^{-4}x^2$	22	1–19	13
$b(17)$	113 127	0.51(5)	0.51	18	1–9 and 17–18	9
$o_3(4)$	113 307	2.5(3)	Q: 2.5	32	1–22	
			$P: 2.5+1.1\times10^{-2}x+1.62\times10^{-5}x^2$			15
$b'(14)$	113 540	18(2)	$P: 18.0-9.1\times10^{-3}x$	40	0–24	15
			$R: 18.0-2.5\times10^{-3}x$			15
$b(18)$	113 707	0.51(6)	0.51	7	4–11	
$b'(15)$	114 169	24(3)	$24-1.0\times10^{-2}x$	41	1–22	
$b(19)$	114 255	0.36(6)	0.36	2	2,8	
$b(20)$	114 746[g]		$P: 5.8-3.6\times10^{-2}x$	6	2–9	
$b'(16)$	114 754	34(4)	$34-2.5\times10^{-2}x$	40	0–24	
$c_3(5)$	114 825[g]	<0.5	$P: 0+2.1\times10^{-2}x$	8	3, 7–13, and 17	13
			$R: 0+7.7\times10^{-3}x$			17
$c'_4(5)$	114 833[g]	0.18	$P: 0+1.6\times10^{-2}x$	15	5–25	17
			$R: 0+2.7\times10^{-2}x$			18
$o_3(5)$	115 259[g]	0.71(8)	Q: 0.71	21	3–17	
			$P: 0.71-8.1\times10^{-3}x+2.1\times10^{-4}x^2$			14
$b'(17)$	115 369	16(2)	16	38	0–23	13
$c_4(0)$	115 566	8.7(9)	Q: 8.7	38	1–22	
			P,R: 8.7			8
$b(22)$	115 663	<0.5		1	9	
$c'_5(0)$	115 850	5.2(6)	$P: 5.2+3.7\times10^{-2}x$	27	5–22	15
			$R: 5.2+1.5\times10^{-2}x$			15
$b(23)$	116 029	0.08(2)		4	4–8	
$b'(18)$	116 206	2.4(3)	$2.4-1.2\times10^{-2}x$	25	0–23	14

[a]Band origin taken from the Harvard CfA N_2 database (Ref. 43).
[b]Present band f-values extrapolated to zero nuclear rotation.
[c]Best fit to band f-values given as a polynomial in $x=J'(J'+1)$.
[d]Total number of observed lines for which reliable f-values could be determined.
[e]The range of J' for which reliable f-values could be determined.
[f]Where the f-value polynomial form is not valid for all measured lines it is restricted to $\le J'_{max}$.
[g]Deduced from this work.

tory of the AIP.[45] Table III lists the newly determined extrapolated, rotationless, band f-values. Also listed are rotationless band f-values derived from CSE calculations[15,17] as well as room temperature band f-values determined by electron energy-loss spectroscopy.[16,32] Comparison with the latter is only appropriate for bands free from significant rotational perturbations.

TABLE II. Summary of predissociation line widths Γ (cm^{-1} FWHM). Uncertainties in units of the last significant digit are given in parentheses.

Level	Γ_0 [a]	$\Gamma(J')$ [b]	Obs. J' [c]
$b'(14)$	0.19(5)	Constant	≤24
$b'(15)$	0.17(3)	$0.17-2.8\times10^{-4}J'(J'+1)$	≤16
$c_3(5)$	0.4(1)	See text	3–13
$c'_4(5)$		See text	7, 9, and 13–19
$o_3(5)$		See text	11–15
$b'(17)$	0.23(2)	See text	≤15

[a]Line widths extrapolated to zero nuclear rotation.
[b]Rotational dependence of line widths.
[c]The range of J' for which line widths have been measured.

Overall, there is reasonable agreement between our rotationless band f-values and the normalized f-values of Geiger and Schröder.[16] The current measurements of the $b(16)-X(0)$ and $b'(13)-X(0)$ bands suggest ~3× larger f-values than determined by Geiger and Schröder[16] and the intervening $c'_4(4)-X(0)$ and $c_3(4)-X(0)$ are much weaker. This may be due to an incorrect partition of the total cross-section across these four bands which are overlapped in the low-resolution spectra of Geiger and Schröder.[16] Also, the f-values of these bands have a strong J' dependence, hampering the comparison of rotationless f-values with a low-resolution experiment. Excluding these four bands, the f-values of Geiger and Schröder[16] are, on average, 18% larger than those determined from the current experiment.

The f-values deduced by Chan *et al.*[32] from their electron energy-loss spectra are consistently higher than our results, by a factor of 1.3–2.7. Our previous publications[20,21] show a similar discrepancy for the N_2 bands at longer wavelengths and provide further discussion. However, no conclusive explanation has been found for the systematic differ-

TABLE III. Comparison of experimental band f-values (in units of 10^{-3}, extrapolated to zero nuclear rotation) with previous experiments and theoretical calculations. Uncertainties in units of the last significant digit are given in parentheses.

Band	This work	Ref. 16[a]	Ref. 32[b]	Ref. 15[a]	Ref. 17[a]
$b(15)-X(0)$	<1	0.52		0.85	1.6
$b'(12)$	16(2)	18	30.3	18	19
$b(16)$	1.1(2)	0.45		1.1	1.3
$c_4'(4)$	18(2)	34	49.6	20	22
$c_3(4)$	<0.3	3.1	2.10	0	0.025
$b'(13)$	10(1)	2.6		11	12
$b(17)$	0.51(5)			2.3	0.83
$o_3(4)$	2.5(3)	2.9	6.20	5.8	3.3
$b'(14)$	18(2)	25	34.1	23	24
$b(18)$	0.51(6)			0.27	0.67
$b'(15)$	24(3)	29	40.9	28	29
$b(19)$	0.36(6)			0.4	0.50
$b'(16)$	34(4)		62.6	38	41
$c_3(5)$	<0.5				
$c_4'(5)$	0.18		0.6	0.4	0.15
$o_3(5)$	0.71(8)		1.55		
$b'(17)$	16(2)	21	31.8	20	21
$c_4(0)$	8.7(9)	12			
$b(22)$	<0.5				
$c_5'(0)$	5.2(6)	5.2		6.5	7.6
$b(23)$	0.08(2)				
$b'(18)$	2.4(3)	1.9	3.26	3.6	2.9

[a]Normalized to $f=0.043$ for $b(3)-X(0)$ (Ref. 20).
[b]Absolute uncertainties ~10%.

ences between the two sets of results. There is a particularly large disagreement between the band f-values of Chan *et al.*[32] and this experiment for $c_3(4)-X(0)$, most likely due to the same resolution effects discussed above regarding the results of Geiger and Schröder.[16]

There is good agreement between the band f-values determined by the current experiment and the coupled-channels modeling of Stahel *et al.*[15] and Spelsberg and Meyer.[17] The present measurements are consistently ~20% lower than modeled by Stahel *et al.*[15] and ~25% below the results of Spelsberg and Meyer.[17] These differences are consistent with the level of agreement found in our previous experiments.[20,21] Unusual disagreement exists for the bands $b(17)-X(0)$ and $o_3(4)-X(0)$, the current measurements yielding only 45% and 26%, respectively, of the oscillator strength modeled by Stahel *et al.*[15] but demonstrating the usual agreement with Spelsberg and Meyer.[17] Similarly, our $b(18)-X(0)$ f-value is twice as large as Stahel *et al.*[15] have predicted. As shown previously,[18] an incorrect relative sign was adopted by Stahel *et al.*[15] for the $o-X$ and $b-X$ diabatic electronic transition moments leading to incorrect CSE model f-values for the $o-X$ transitions and their perturbation partners.

Also included in the accompanying data archive[45] are f-value measurements for the $b'(3)-X(0)$ band. This is in the interest of completeness regarding a previous publication[20] in this series of reports.

The following paragraphs provide a band-by-band summary of our observations. Unless noted otherwise, it can be assumed that the relevant predissociation line widths are $\lesssim 0.1$ cm^{-1} FWHM, the minimum detectable line width.

A. $b(15)-X(0)$

Multiple lines from this band are visible for $J' \leq 10$ but are all weak or blended and only an upper limit on the rotationless band f-value could be determined. However, a few higher-rotation lines ($J'=15-20$) with greater strength appear among the lines of the $b'(11)-X(0)$ band. The f-values of these lines have been measured and show no discernible branch dependence.

B. $b'(12)-X(0)$

Rotational lines have been observed up to $J'=16$ in the P branch and $J'=21$ in the R branch. A weak linear J' dependence of band f-values is observed with no detectable difference between the two branches.

C. $b(16)-X(0)$

This weak band appears amid the high-rotational lines of $c_4'(4)-X(0)$. The f-values of six lines between $J'=2$ and 9 have been measured and additional weak lines are identifiable. The quality of the data does not permit the identification of any J' dependence for the band f-values and a weighted mean of all measurements has been assumed as the best rotationless estimate.

D. $c_4'(4)-X(0)$

This strong band shows a 60% increase in band f-value between $J'=0$ and 15, falling off thereafter, with measurable transitions being observed as far as $J'=23$. The initial in-

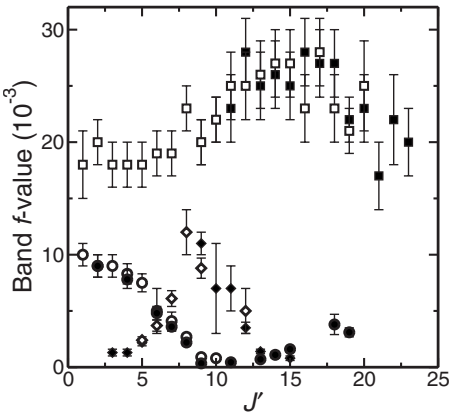

FIG. 1. Band f-values for the transitions $c_4'(4)-X(0)$ (squares), $c_3(4)-X(0)$ (diamonds), and $b'(13)-X(0)$ (circles). P-branch f-values are shown as open symbols and R-branch values as closed.

crease in band f-value explains why the $J'=0$ value measured in this experiment is less than the band-averaged f-value of Geiger and Schröder.[16]

The three excited levels $c_4'(4)$, $c_3(4)$, and $b'(13)$ are strongly coupled, forming a complex of bands which has been studied previously by Yoshino *et al.*[46] and Walter *et al.*[42] Figure 2 of Ref. 42 shows the term values of the coupled upper states of the complex and our band f-value measurements are reproduced in Fig. 1. All three term series clearly deviate from the straight lines characteristic of unperturbed bands when plotted against $J'(J'+1)$, and the band f-values are highly J'-dependent.

The intensity patterns of these bands have no straightforward explanation, due to the complexity of the upper-state interactions. The photofragment intensities measured by Walter *et al.*,[42] following excitation from the $a''\,{}^1\Sigma_g^+$ metastable state, are not directly comparable to f-values of transitions from the ground state but show a similar degree of rotational variation.

Helm *et al.*[36] measured rotationally resolved line widths for $c_4'(4)$, which increase from 0.016 cm^{-1} FWHM at $J'=1$ to 0.17 cm^{-1} FWHM at $J'=19$. No line broadening was observed in the current experiment even though the greatest line widths of Helm *et al.*[36] should be detectable.

E. $c_3(4)-X(0)$

Yoshino *et al.*[46] assigned the rotational series of $c_3(4)$ and $b'(13)$ so that they cross near $J'=9$ whereas Walter *et al.*[42] adopted an adiabatic assignment of term values as is done here. The P- and R-branch lines are easily observed, while the Q branch is entirely absent. Evidently, the P and R lines borrow their intensity from transitions to the surrounding $^1\Sigma_u^+$ states. Therefore, this band has insufficient intrinsic strength to be detected by the present experiment and appears purely because it is perturbed by the e-parity levels of the $^1\Sigma_u^+$ states for $J'>0$. For this reason, no rotationless f-value could be determined directly and only an upper limit is listed in Tables I and III.

The P- and R-branch f-values increase quadratically with $J'(J'+1)$ as far as $J'=8$. Following the avoided crossing with $b'(13)$ at $J'\sim 9$, the transitions to $c_3(4)$ rapidly decrease in strength and are observed up to $J'=15$. The $c_3(4)$ line widths determined by Helm *et al.*,[36] extending to $J'=13$, are all <0.1 cm^{-1} FWHM and below the minimum detectable line width of our experiment.

F. $b'(13)-X(0)$

R-branch lines were observed up to $J'=19$ and P-branch lines up to $J'=10$. Because of increasing rotational mixing with $c_3(4)$, the band f-values of $b'(13)-X(0)$ decrease rapidly up to $J'=8$ and then increase again. The experimental band f-values of Geiger and Schröder[16] are not comparable to our extrapolated rotationless f-values because of this J' dependence. No line broadening of $b'(13)$ was detected, which is consistent with the experimental line widths determined by Helm *et al.*[36] of ~ 0.07 cm^{-1} FWHM for $J'=3-5$.

G. $b(17)-X(0)$

Twenty-one unblended lines, all for $J'\leq 9$, were measured. These lines show no J' or branch dependence and a weighted mean of all band f-values is taken as the estimated rotationless f-value, 0.51×10^{-3}. Additionally, high-rotational R-branch lines are visible among the lines of the stronger $b'(13)-X(0)$ band, two of which $(J'=18,19)$ have been fitted and show much larger band f-values, 7.1×10^{-3} and 5.9×10^{-3}, respectively. This perturbation likely points to a level crossing and rotational mixing with $b'(13)$ at $J'\sim 18$.

H. $o_3(4)-X(0)$

Transitions up to $J'=22$ were observed in both the e- and f-parity levels. An energy level perturbation, and resultant line strength sharing with $b'(14)-X(0)$, indicates a level crossing in the term series of $o_3(4)$ and $b'(14)$ between $J=17$ and 18 [see also the section on $b'(14)-X(0)$]. The current assignments[45] of e-parity levels for $J'=20$ and 21 differ from previous values[47] with two blended lines at 132 380 cm^{-1} newly distinguishable because of an asymmetrical combined line shape.

Because of intensity sharing with $b'(14)-X(0)$, the experimental band f-values cannot be wholly constrained by a polynomial form in Table I and are plotted in Fig. 2. The Q-branch band f-values are unaffected by this perturbation and are clearly J' independent. The lowest-J' lines of the P and R branches converge to the same band f-value as the Q branch. The P-branch band f-values do, however, show a quadratic increase with $J'(J'+1)$ as far as $J'=18$. The R branch is blended for $2\leq J'\leq 12$ and band f-values for $J'=13$ and 14 are weaker than the Q-branch f-values, while the P branch is somewhat stronger. Stronger R-branch lines were also measured for $J'=20-22$.

I. $b'(14)-X(0)$

This band has been followed as far as $J'=19$ in the P branch and $J'=24$ in the R branch. The measured band f-values (plotted in Fig. 2) are constant for low J'. However, the P branch loses strength for $J'=17-18$ and the R branch

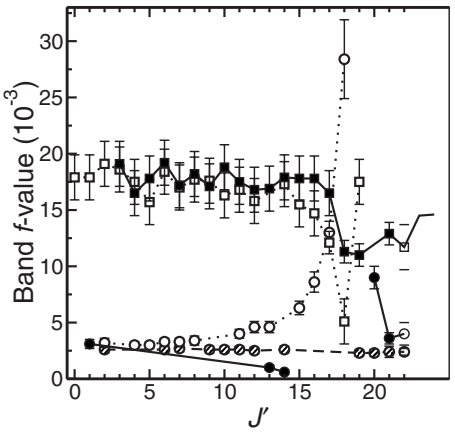

FIG. 2. Band f-values for the transitions $o_3(4)-X(0)$ (circles) and $b'(14)-X(0)$ (squares). P-branch f-values are shown as open symbols joined by dotted lines, the R-branch values as closed symbols joined by solid lines, and the Q-branch values as hashed symbols joined by dashed lines.

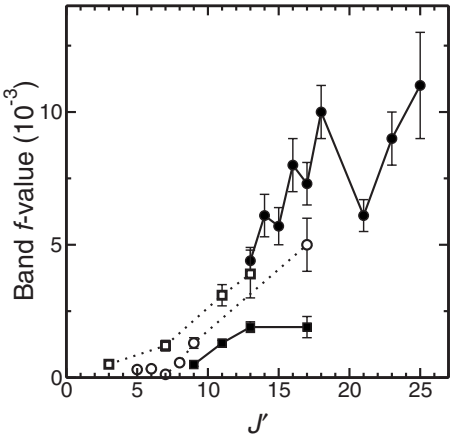

FIG. 3. Band f-values of the transitions $c_4'(5)-X(0)$ (circles) and $c_3(5)-X(0)$ (squares). P-branch f-values are shown as open symbols joined by dotted lines, the R-branch values as closed symbols joined by solid lines.

shows weakened lines for $J'=18-19$. There is a rapid change in the relative strengths of the P and R branches at the crossing point with $o_3(4)-X(0)$ (between $J'=18$ and 19) and the approximately inverse behavior is shown by the f-values of $o_3(4)-X(0)$. This is indicative of the sharing of intensity between transitions of types $\Pi-\Sigma$ and $\Sigma-\Sigma$.[48,49] The highest P- and R-branch lines are seen to be reverting to their unperturbed f-values.

It was possible to measure the widths of many $b'(14)-X(0)$ lines. These were found to be independent of J', with a mean value of 0.19 ± 0.05 cm^{-1} FWHM.

J. $b(18)-X(0)$

Many lines from all three branches are visible in our spectra, though only a subset of these, $J'=4-11$ in the Q branch and $J'=7$ in the P branch, are unblended and strong enough to be analyzed. No J' dependence in the band f-values was detected.

K. $b'(15)-X(0)$

Strong P and R branches are followed to $J'=21$ and 22, respectively, with f-values gradually decreasing. We also tentatively suggest that the R branch is slightly stronger than the P branch for high J'. Measured line widths are found to decrease approximately linearly with $J'(J'+1)$ from 0.17 ± 0.03 cm^{-1} at $J'=0$ to below the measurable limit of ~0.1 cm^{-1} by $J'=16$.

L. $b(19)-X(0)$

This weak band appears at the tail end of the $b'(16)-X(0)$ spectrum. Many lines are visible but only two of them, $J'=2$ and 8 in the Q branch, could be quantified. The mean of these two lines is taken as the best estimate of the rotationless band f-value.

M. $b(20)-X(0)$

Weak lines appearing amid the strong $b'(16)-X(0)$ band have been assigned to $b(20)-X(0)$. Sixteen lines in the P and R branches have been identified, with line energies and e-parity term values listed in the EPAPS data archive.[45] Molecular parameters were calculated from these term values, giving $T_0=114745.76\pm0.5$, $B=1.07\pm0.02$, $D=(7\pm2)\times10^{-4}$, and $H=(10\pm5)\times10^{-7}$ cm^{-1}.

Band f-values of P-branch lines for $J'=2-4$ and 7–9 are found to scatter widely, apparently decreasing with increasing J'. We have not determined a rotationless f-value from these measurements, the P-branch f-values very likely being influenced by an interaction with $b'(16)$.

Many of the lines attributed to this band have been previously noted but not assigned.[43] The $b(20)-X(0)$ lines are interspersed with higher-rotational lines of $c_4'(5)-X(0)$ and $c_3(5)-X(0)$, which are also newly assigned. It has been possible to partition the observed features between these three bands by requiring continuity of the analyzed band f-values.

N. $b'(16)-X(0)$

This is the strongest band in the spectral region covered by this publication with 40 lines measured, progressing up to $J'=24$. These exhibit a gradual decrease in band f-value with no apparent divergence of the P and R branches.

O. $c_3(5)-X(0)$

This band has been assigned rotationally for the first time,[45] but many of the lines attributed to it have been detected previously.[43] It is overlapped by $c_4'(5)-X(0)$, and both bands appear weakly in the windows of $b'(16)-X(0)$ for high J'.

The energies and strengths of rotational lines arising from the transitions $c_n(v)-X(0)$ and $c_{n+1}'(v)-X(0)$ may be analyzed according to the formalism of a p-complex. However, for $n=3$ and $v=5$, interactions with the valence states $b\,^1\Pi_u$ and $b'\,^1\Sigma_u^+$ cause significant perturbations and, here, the $c_3(5)-X(0)$ and $c_4'(5)-X(0)$ bands are treated separately.

The $c_3(5)-X(0)$ band f-values, shown in Fig. 3, are strongly J'-dependent. The measured R-branch f-values show a large increase between $J'=9$ and 13, and the P-branch f-values show a tenfold increase between $J'=3$ and

13 and are ~2 times stronger than the R branch. No Q-branch lines could be definitively assigned in the spectrum.

Term values were determined for 15 e-parity levels between $J'=3$ and 19; they are reproduced by the parameters $T_0=114\,825\pm2$, $B=1.42\pm0.05$, $D=(-9\pm2)\times10^{-4}$, and $H=(-1.1\pm0.5)\times10^{-6}$ cm^{-1}, with an accuracy of 0.5 cm^{-1}.

The mean measured line width for $J'=3$ and 7 is 0.4 ± 0.1 cm^{-1} FWHM, and is the best estimate of a rotationless value. The line width decreases to a mean value of 0.20 ± 0.05 cm^{-1} FWHM for $J'=9,11$ and 13.

P. $c_4'(5)-X(0)$

Carroll *et al.*[50] report the molecular parameters $T_0=114\,830.2$ and $B=1.8$ cm^{-1} for $c_4'(5)$ but it appears that no rotational assignments have been published. The spectra analyzed here have resulted in new assignments for 14 R-branch lines ($J'=11-24$) and seven P-branch lines ($J'=6-10,18,20$). Line positions and the resultant term values are listed in the EPAPS data archive[45] and experimental band f-values are plotted in Fig. 3.

Because the lowest-rotation experimental term value has $J'=5$, and $c_4'(5)$ is very near to the $c_3(5)$ perturber, it is not possible to determine the band origin with much accuracy. Molecular parameters were determined employing term values with $J'\leq18$, giving $T_0=114\,833\pm2$, $B=1.66\pm0.04$, $D=(-5\pm3)\times10^{-4}$, and $H=(-8\pm5)\times10^{-7}$ cm^{-1}. Higher-J' term values are not included, $J'=21$ being pushed downwards by ~8 cm^{-1} and $J'=22$ being pushed upwards by ~3 cm^{-1}. The cause of this is likely to be a level crossing with $b(21)$, although no extra lines could be unambiguously assigned to a $b(21)-X(0)$ transition.

An incomplete series of band f-values was measured between $J'=5$ and 25 showing a rapid increase as far as $J'=18$. There is a decrease for $J'=21$, with regained strength for $J'=23$ and 25, which is consistent with the occurrence of intensity sharing with $b(21)-X(0)$. The mean of the lowest-J' f-values was adopted as a rotationless value.

The $c_4'(5)$ line widths were determined to be significant and variable, increasing from 0.22 ± 0.09 to 0.91 ± 0.06 cm^{-1} FWHM between $J'=5$ and 7. Very likely $P(J'=9)$ is even broader but could not be measured. There is a gap in the measurements for $J'\leq13$, after which the line widths decrease substantially and fall below the measurable limit of 0.1 cm^{-1} FWHM by $J'=20$.

Q. $o_3(5)-X(0)$

It has been possible to make the first assignments of heavily-mixed members of the $o_3(5)-X(0)$ Q branch ($J'=3-12$), as well as higher-rotational lines of the P and R branches ($J'=8-17$), with transition energies and term values listed in the EPAPS data archive.[45]

From f-parity levels the following parameters have been derived: $T_0=115\,258.8\pm1$, $B=1.01\pm0.01$ and $D=(-2.5\pm0.1)\times10^{-3}$ cm^{-1}. The very low B and large negative D values result from a crossing at low J' of the Rydberg $o_3(5)$ level by the higher-lying valence level $b(21)$. Thus, the lowest observed adiabatic levels have principally

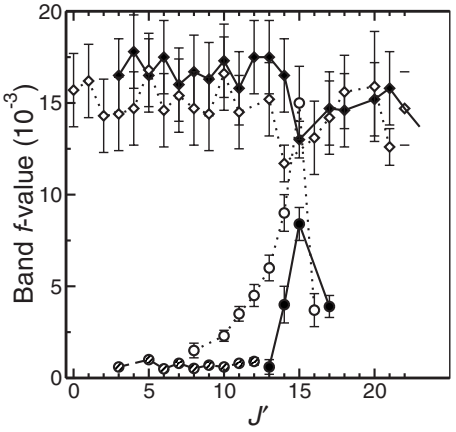

FIG. 4. Band f-values of the transitions $o_3(5)-X(0)$ (circles) and $b'(17)-X(0)$ (diamonds). P-branch f-values are shown as open symbols joined by dotted lines, the R-branch as closed symbols joined by solid lines, and the Q-branch as hashed symbols joined by dashed lines.

$b(21)$ character, reverting to $o_3(5)$ at higher J'. The Q-branch band f-values show a large degree of scatter because they are close to the noise level of the measurement and no variation with J' is discernible despite the expected interaction with $b(21)$. No lines from the complementary adiabatic transition [$b(21)-X(0)$ at higher J'] have been positively identified although there are a few weak lines remaining unassigned in the spectrum.

The P and R branches appear much more strongly than the Q branch because of a level crossing with $b'(17)$ between $J'=15$ and 16. Intensity borrowing from the much stronger $b'(17)-X(0)$ band results in rapidly varying band f-values for both bands, plotted in Fig. 4. The $o_3(5)-X(0)$ P branch appears more strongly than the R branch for J' below the crossing point and the reverse is true for higher J'. A similar P/R intensity interference effect resulting from a rotational perturbation is discussed in the section concerning $b'(14)-X(0)$.

The J'-dependent broadening of the e-levels reaches a maximum of 0.57 ± 0.12 cm^{-1} FWHM at $J'=12$ and decreases for higher J'.

R. $b'(17)-X(0)$

This strong band was analyzed as far as $J'=21$ and 23 in the P and R branches, respectively, and for $J'\leq13$ the measured band f-values (plotted in Fig. 4) are unperturbed, except for the P being slightly weaker than the R branch. The $J'=14$ P-branch f-value is reduced due to the crossing with $o_3(5)$ discussed in the previous section and the same is observed for $J'=15$ in the R branch.

This band is broadened by predissociation. The average width of lines having $J'\leq5$ is 0.23 ± 0.05 cm^{-1} FWHM. The width decreases to 0.1 cm^{-1} FWHM for $J'=9$ and increases again for 13 to 15.

S. $c_4(0)-X(0)$

The upper level of this band is strongly rotationally coupled to $c_5'(0)$, as well as being weakly perturbed by $b(22)$ with an observed level crossing between $J'=8$ and 9. This

complex of three bands has been studied previously by Yoshino and Freeman[51] and Helm and Cosby[39] and the behavior of the band f-values determined here is in agreement with the mutual perturbations discussed by these authors.

The Q branch of this band is free from the e-level perturbation by $c_5'(0)$ and has been observed up to $J'=22$, with a constant band f-value. The perturbation by $b(22)$ is revealed by energy shifts in the $J'=8$ and 9 term values.

There is significant $c_4(0)$ Λ-doubling with e-parity levels 30 cm^{-1} below the f-parity levels at $J=20$ because of the higher-lying perturber $c_5'(0)$. A dip in both P- and R-branch band f-values at $J'=9$ is observed, resulting from the perturbation by $b(22)$. Extra lines attributable to $b(22)-X(0)$ appear in the spectrum. Otherwise, for $J' \leq 14$ the P- and R-branch band f-values mirror the Q-branch values, but there is a clear increase in R-branch line strength and decrease in the P-branch for $J' > 14$. The reverse P/R line strength pattern is observed in the $c_5'(0)-X(0)$ band f-values.

T. $b(22)-X(0)$

This band appears in our experimental spectra but is too weak to be analyzed reliably, except for the $J'=9$ P- and R-branch lines which borrow significant strength because of a level crossing with $c_4(0)$. These two lines are identifiable by a reliable combination difference.[51] The R-branch line is blended, but the P-branch line has been measured to have a strength comparable to that lost by the corresponding $c_4(0)-X(0)$ line. Only an upper limit can be placed on the rotationless band f-value, based on the noise level of the spectra in the region where the $b(22)-X(0)$ band head is located.

U. $c_5'(0)-X(0)$

Lines have been measured for $5 \leq J' \leq 21$. The band f-values of both branches increase up to $J' \sim 16$, at which point the P-branch f-values are twice as large as the R-branch values. At higher J', the P-branch f-values remain constant and the R-branch values decrease.

V. $b(23)-X(0)$

Only a few lines of this band are discernible above the background noise, and in some cases these are overlapped with lines of $b'(18)-X(0)$, their presence being suggested by the resultant blends which are too strong to be attributed purely to $b'(18)-X(0)$. The measured band f-values are too few and too widely scattered for conclusions to be drawn concerning the relative strengths of the P, Q, and R branches of $b(23)-X(0)$ and possible J'-dependencies. The mean band f-value for the four measured lines is given in Table I.

W. $b'(18)-X(0)$

In this strong band, f-values rapidly decrease with J' in both the P and R branches, which disappear altogether in our spectra by $J'=15$. There is a resurrection of line strength after this, with measurable R-branch lines for $J'=19-22$ and additional R- and P-branch lines clearly visible but too weak to be parameterized. This analysis has resulted in some new high-rotational assignments listed in the accompanying data archive.[45]

ACKNOWLEDGMENTS

Partial support for this research was provided by the Australian Research Council Discovery Program through Grant No. DP0558962 and by NASA Grant No. NNX08AE786 to Wellesley College. The measurements were carried out under the approval of the Photon Factory Advisory Committee (Proposal No. 1998G245). We thank the staff of the Photon Factory for their hospitality and assistance.

[1] P. D. Feldman, D. J. Sahnow, J. W. Kruk, E. M. Murphy, and H. W. Moos, J. Geophys. Res. **106**, 8119 (2001).
[2] J. Bishop, M. H. Stevens, and P. D. Feldman, J. Geophys. Res. **112**, A10312 (2007).
[3] D. F. Strobel and D. E. Shemansky, J. Geophys. Res. **87**, 1361 (1982).
[4] M. H. Stevens, R. R. Meier, R. R. Conway, and D. F. Strobel, J. Geophys. Res. **99**, 417 (1994).
[5] J. M. Ajello, M. Joseph, M. H. Stevens, I. Stewart, K. Larsen, L. Esposito, J. Colwell, W. McClintock, G. Holsclaw, J. Gustin, and W. Pryor, Geophys. Res. Lett. **34**, L24204 (2007).
[6] A. L. Broadfoot, S. K. Atreya, J. L. Bertaux, J. E. Blamont, A. J. Dessler, T. M. Donahue, W. T. Forrester, D. T. Hall, F. Herbert, J. B. Holberg, D. M. Hunten, V. A. Krasnopolsky, S. Linick, J. I. Lunine, J. C. McConnell, H. W. Moos, B. R. Sandel, N. M. Schneider, D. E. Shemansky, G. R. Smith, D. F. Strobel, and R. V. Yelle, Science **246**, 1459 (1989).
[7] M.-C. Liang, A. N. Heays, B. R. Lewis, S. T. Gibson, and Y. L. Yung, Astrophys. J. **664**, L115 (2007).
[8] V. Vuitton, R. V. Yelle, and V. G. Anicich, Astrophys. J. **647**, L175 (2006).
[9] F. Bakalian, Icarus **183**, 69 (2006).
[10] F. Bakalian and R. E. Hartle, Icarus **183**, 55 (2006).
[11] J. L. Fox, Icarus **192**, 296 (2007).
[12] H. Lefebvre-Brion, Can. J. Phys. **47**, 541 (1969).
[13] K. Dressler, Can. J. Phys. **47**, 547 (1969).
[14] P. K. Carroll and C. P. Collins, Can. J. Phys. **47**, 563 (1969).
[15] D. Stahel, M. Leoni, and K. Dressler, J. Chem. Phys. **79**, 2541 (1983).
[16] J. Geiger and H. Schröder, J. Chem. Phys. **50**, 7 (1969).
[17] D. Spelsberg and W. Meyer, J. Chem. Phys. **115**, 6438 (2001).
[18] B. R. Lewis, S. T. Gibson, W. Zhang, H. Lefebvre-Brion, and J. M. Robbe, J. Chem. Phys. **122**, 144302 (2005).
[19] J. P. Sprengers, E. Reinhold, W. Ubachs, K. G. H. Baldwin, and B. R. Lewis, J. Chem. Phys. **123**, 144315 (2005).
[20] G. Stark, K. P. Huber, K. Yoshino, P. L. Smith, and K. Ito, J. Chem. Phys. **123**, 214303 (2005).
[21] G. Stark, B. R. Lewis, A. N. Heays, K. Yoshino, P. L. Smith, and K. Ito, J. Chem. Phys. **128**, 114302 (2008).
[22] V. E. Haverd, B. R. Lewis, S. T. Gibson, and G. Stark, J. Chem. Phys. **123**, 214304 (2005).
[23] J. P. Sprengers and W. Ubachs, J. Chem. Phys. **122**, 144301 (2005).
[24] T. Hashimoto and H. Kanamori, J. Mol. Spectrosc. **235**, 104 (2006).
[25] B. R. Lewis, K. G. H. Baldwin, J. P. Sprengers, W. Ubachs, G. Stark, and K. Yoshino, J. Chem. Phys. **129**, 164305 (2008).
[26] B. R. Lewis, A. N. Heays, S. T. Gibson, H. Lefebvre-Brion, and R. Lefebvre, J. Chem. Phys. **129**, 164306 (2008).
[27] X. Liu, D. E. Shemansky, C. P. Malone, P. V. Johnson, J. M. Ajello, I. Kanik, A. N. Heays, B. R. Lewis, S. T. Gibson, and G. Stark, J. Geophys. Res. **113**, A02304 (2008).
[28] M. A. Khakoo, C. P. Malone, P. V. Johnson, B. R. Lewis, R. Laher, S. Wang, V. Swaminathan, D. Nuyujukian, and I. Kanik, Phys. Rev. A **77**, 012704 (2008).
[29] V. L. Carter, J. Chem. Phys. **56**, 4195 (1972).
[30] P. Gurtler, V. Saile, and E. E. Koch, Chem. Phys. Lett. **48**, 245 (1977).
[31] R. D. Hudson and V. L. Carter, J. Opt. Soc. Am. **58**, 227 (1968).
[32] W. F. Chan, G. Cooper, R. Sodhi, and C. E. Brion, Chem. Phys. **170**, 81 (1993).
[33] W. Ubachs, I. Velchev, and A. de Lange, J. Chem. Phys. **112**, 5711

(2000).
[34] W. Ubachs, K. S. E. Eikema, and W. Hogervorst, Appl. Phys. B: Lasers Opt. **57**, 411 (1993).
[35] J. P. Sprengers and W. Ubachs, J. Mol. Spectrosc. **235**, 176 (2006).
[36] H. Helm, I. Hazell, and N. Bjerre, Phys. Rev. A **48**, 2762 (1993).
[37] B. Buijsse and W. J. van der Zande, Phys. Rev. Lett. **79**, 4558 (1997).
[38] B. Buijsse and W. J. van der Zande, Faraday Discuss. **108**, 271 (1997).
[39] H. Helm and P. C. Cosby, J. Chem. Phys. **90**, 4208 (1989).
[40] C. W. Walter, P. C. Cosby, and H. Helm, J. Chem. Phys. **99**, 3553 (1993).
[41] C. W. Walter, P. C. Cosby, and H. Helm, Phys. Rev. A **50**, 2930 (1994).
[42] C. W. Walter, P. C. Cosby, and H. Helm, J. Chem. Phys. **112**, 4621 (2000).
[43] Harvard-Smithsonian CfA N_2 online archive (http://www.cfa.harvard.edu/amp/ampdata/N2ARCHIVE/n2home.html) (2008).
[44] G. Herzberg, *Molecular Structure and Molecular Spectra I. -Spectra of Diatomic Molecules* (Krieger, Florida, 1989), p. 208.
[45] See EPAPS supplementary material at http://dx.doi.org/10.1063/1.3257690. This data archive consists of tabulations of experimentally determined $^{14}N_2$ line and band f-values for 23 bands between 86.0 and 89.7 nm. Also included are line widths for 6 bands, and transition energies and term values for 11 bands.
[46] K. Yoshino, D. E. Freeman, and Y. Tanaka, J. Mol. Spectrosc. **76**, 153 (1979).
[47] K. Yoshino, Y. Tanaka, P. K. Carroll, and P. Mitchell, J. Mol. Spectrosc. **54**, 87 (1975).
[48] R. A. Gottscho, J. B. Koffend, R. W. Field, and J. R. Lombardi, J. Chem. Phys. **68**, 4110 (1978).
[49] H. Lefebvre-Brion and R. W. Field, *The Spectra and Dynamics of Diatomic Molecules* (Elsevier, New York, 2004), pp. 386–396.
[50] P. K. Carroll, C. P. Collins, and K. Yoshino, J. Phys. B **3**, L127 (1970).
[51] K. Yoshino and D. E. Freeman, Can. J. Phys. **62**, 1478 (1984).